High Pressure Research
Vol. 26, No. 3, September 2006, 145–163

Taylor & Francis
Taylor & Francis Group

Superconductivity in the alkali metals

J. S. SCHILLING*

Department of Physics, Washington University, CB 1105, One Brookings Dr, St. Louis, MO 63130, USA

(Received 3 May 2006; revised 4 June 2006; in final form 18 June 2006)

At ambient pressure there are 29 elemental superconductors in the periodic table, none of which is an alkali metal. The first alkali metal to become superconducting under high pressure is Cs followed years later by Li. Alkali metals are believed to be exemplary free-electron systems. The fact that an alkali metal becomes superconducting at all is surprising and is a result of the fact that under pressure it shows marked deviations from free-electron behaviour where, counterintuitively, bands narrow and gaps widen. For this reason the alkali metals are among the most interesting systems known to study in high-pressure experiments and superconductivity is one of their most fascinating properties.

Keywords: Superconductivity; Alkali metals; High pressure

1. Introductory remarks

The alkali metals grace the first column of the periodic table and range from the *potential* alkali metal, hydrogen (H), to the *neglected* alkali metal, francium (Fr), with lithium (Li), sodium (Na), potassium (K), rubidium (Rb) and cesium (Cs) lying in between. No alkali metal is known to superconduct at ambient pressure. However, element number one, hydrogen, an excellent electrical insulator in condensed form, will almost certainly become an alkali metal if exposed to extreme pressures, possibly exhibiting superconductivity at near ambient temperatures [1]. The properties of solid Fr are likely quite similar to those of Cs. However, the highly radioactive Fr is the most unstable of the first 103 elements in the period table, its longest lived isotope having a half life of only 22 minutes. There is at most one ounce of Fr in the entire earth at any given instant in time (see [2]). Although no weighable amounts of Fr have ever been accumulated, magneto-optic techniques have succeeded in trapping a sufficient number of atoms to allow studies of its optical properties [3].

Whereas Fr may be the rarest element on earth, H, a potential alkali metal, is by far the most abundant element in the visible universe, making up more than 90% of all atoms. H is a very special element by virtue of the fact that it is the lightest and possesses no electron core. The richness of the properties that H is predicted to exhibit under extreme pressures has likely

*Email at http://waphys.wostl.edu

High Pressure Research
ISSN 0895-7959 print/ISSN 1477-2299 online © 2006 Taylor & Francis
http://www.tandf.co.uk/journals
DOI: 10.1080/08957950600864401

no equal among all condensed matter systems. As if the prospect of superconductivity near room temperature were not enough, at sufficient densities the alkali metal H may choose a fluid phase for its ground state where the superconductivities of proton–proton and electron–electron Cooper pairs may coexist [4]. This raises the possibility of a superflow of mass, but not charge, if the proton–proton and electron–electron pairs flow in the same direction with equal velocity [5]; a recent numerical experiment has even raised the prospect of a novel type of quantum ordered state that features superfluidity with Ohmic resistance if the proton and electron pairs flow in opposite directions, a 'metallic superfluid' [6]!

Unfortunately, experiments on H_2 have thus far been limited to pressures of order 300 GPa [7, 8] – insufficient to transform this insulating molecular solid into an alkali metal at ambient temperatures and below. For this transformation, pressures near 400 GPa [9] or above are required. However, we note that a continuous transition of H_2 from a semiconducting to a metallic diatomic fluid at 140 GPa and 3000 K has been reported in shockwave experiments [10]. Recent advances in the synthesis of artificial diamonds may push the experimentally available pressure range in diamond-anvil cells upward [11, 12]. Another strategy to reduce the metallization pressure is to expose hydrogen to chemical pressure by incorporating it into compounds, in particular hydrides of the group-IVa elements C, Si and Ge [13]. In a recent paper Feng *et al.* [14] have predicted that SiH_4 should become metallic at pressures near 'only' 90 GPa.

The monovalent metals consist of the alkali metals and the noble metals, none of which are superconducting at ambient pressure. The alkali metals, in particular, are generally believed to be the metals which most closely obey the simple nearly-free-electron model pioneered by Wigner and Seitz [15]. Indeed, their Fermi surfaces are nearly spherical, reflecting the weak electron–ion scattering (pseudopotential). In view of this and the low electronic density of states at the Fermi surface, the absence of superconductivity at ambient pressure is not surprising. In Li, for example, conventional electronic structure calculations place the superconducting transition temperature near $T_c \approx 1$ K [16], whereas a more sophisticated calculation, which treats electron–electron repulsive and attractive interactions on an even footing, estimates $T_c \approx 0.4$ mK [17]. Indeed, no experimental evidence has been found for superconductivity in Li above 100 μK [18].

If an alkali metal is not superconducting at ambient pressure, would one expect it to become superconducting under high pressure? Assuming electron–phonon coupling between nearly free electrons, the answer is unequivocal: NO. As every elementary textbook on solid state physics emphasizes, bringing the atoms of a solid closer together broadens the bands and reduces energy gaps. For this reason all insulators will eventually become metals under sufficient compression. In metals the broadening of the bands reduces the electronic density of states at the Fermi energy $N(E_f)$; for a 3D free electron gas, $N(E_f) \propto V^{2/3}$. This, together with increasing lattice stiffening under pressure, leads to a reduction in the strength of the electron–phonon coupling (see, for example, [19, 20]). It is thus not surprising that, without exception, superconductivity in all simple (s, p-electron) metals is weakened if high pressures are applied, as evidenced by the negative pressure derivatives dT_c/dP for Pb, Al, In, Sn, etc. Within the nearly-free-electron model, therefore, a simple metal that is not superconducting under ambient conditions, such as the alkali metals, would *not* be expected to become superconducting under high pressure. That this simple picture breaks down is seen from the fact that the canonical free-electron metals Cs and Li both become superconducting under sufficiently high pressures. In fact, the electronic-structure calculations of Boettger and Trickey [21] predict that a sizeable *narrowing* of the bands near the Fermi surface occurs if Li is strongly compressed, in sharp contrast to free-electron theory. In addition, a recent *ab initio* electronic structure calculation finds that Li's Fermi surface becomes increasingly anisotropic with pressure, contacting the zone boundary at the relatively moderate pressure

of ∼8 GPa [22, 23]. This clearly shows that the above simple free-electron picture has limited validity when an alkali metal is strongly compressed.

We now examine more carefully what changes occur in the electronic properties of an alkali metal under progressively higher pressures. As seen in figure 1, the alkali metals possess an extraordinarily high compressibility, rivaling that of H_2. In the simple free-electron picture for a monovalent metal with a *bcc* cubic lattice and lattice parameter a, the Fermi sphere is completely contained within the 1st Brillouin zone, the Fermi wavevector $k_f = (6\pi^2)^{1/3}/a$ reaching out 88% of the distance to the nearest zone boundary at $d_{zb} = \sqrt{2}\pi/a$. As the lattice parameter decreases under pressure, both the Fermi sphere and first Brillouin zone expand at the same rate, so that one never crosses the other, i.e. the diffraction condition is never satisfied.

In this simple free-electron picture it is tacitly assumed that the conduction electrons are free to wander *throughout* the crystal lattice. In fact, the Pauli exclusion principle and wavefunction orthogonality requirements prevent the conduction electrons from penetrating into the atomic core region with volume V_c, forcing them to dwell in the *interstitial* regions [33, 34]. This leads to a reduction in the free volume available to the conduction electrons. The free-electron properties are strongly modified not only due to the rapidly shrinking free volume, but also because the shape of the interstitial regions to which they are confined is not spherical, but highly irregular. This promotes the relative importance of the higher angular momentum components of the electronic wavefunctions, *i.e.* pressure-induced $s \rightarrow p$ or $s \rightarrow d$ transfer, through which, respectively, the p-band occupancy n_p or the d-band occupancy n_d increases. Pressure-induced $s \rightarrow d$ transfer for the alkali metal Cs is clearly seen in the qualitative energy band diagram in figure 2, where for pressures above ∼3 GPa the bottom of the $5d$-band falls below the Fermi energy E_f (horizontal dashed line) located in the $6s$-band, *i.e.* Cs begins to become a transition metal. The d-band occupancy n_d has been shown to be the single most important factor in determining the crystal structure at ambient and high pressures across the transition metal and rare-earth series [35] and likely plays an important role in the structural and superconducting properties of the heavier alkali metals K, Rb and Cs.

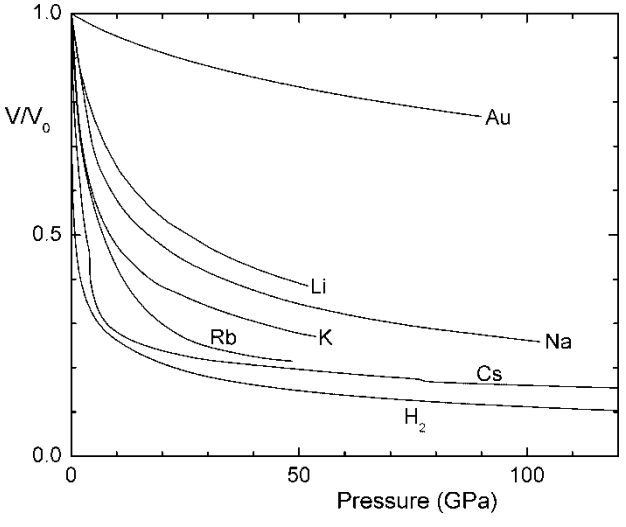

Figure 1. Equations of state to 50–120 GPa pressure for hydrogen [24, 25], lithium [26, 27], sodium [28], potassium [29], rubidium [29] and cesium [30, 31]. For comparison, the equation of state of gold is also shown [32], chosen to represent a typical noble metal or transition metal. All data were obtained at room temperature except for lithium above 21 GPa (160–200 K) and hydrogen below 10 GPa (5 K).

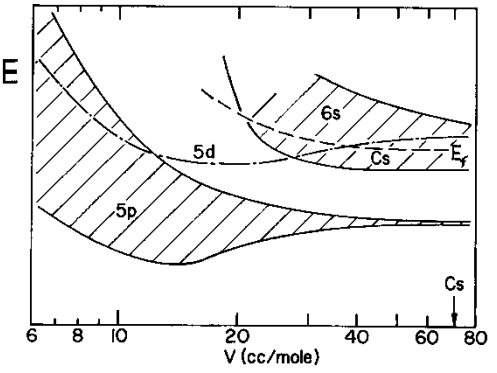

Figure 2. Sketch of the energy bands for Cs as a function of molar volume V. The molar volume at ambient pressure is $V_o \simeq 71\,\mathrm{cm\,mole^{-1}}$ from [36]. (Values of the ionic radius r_c and volume per atom V_a at ambient pressure are taken from ref. [36]. For Y^{3+}, Sc^{3+}, La^{3+}, Lu^{3+}, Li^{1+}, Na^{1+}, K^{1+}, Rb^{1+}, Cs^{1+} we find, respectively, $r_c = 0.90$, 0.75, 1.03, 0.86, 0.76, 1.02, 1.38, 1.52, 1.67 Å and $r_a \equiv \sqrt[3]{(3/4\pi)V_a)} = 1.99$, 1.84, 2.08, 1.92, 1.73, 2.11, 2.62, 2.81, 3.04 Å.) As pressure is applied and V is reduced, $s \rightarrow d$ transfer begins near $35\,\mathrm{cm^3\,mole^{-1}}$ (∼3 GPa) when the bottom of the 5d-band slides below the Fermi energy E_f and ends when the bottom of the 6s band rises above E_f near $20\,\mathrm{cm^3\,mole^{-1}}$ (∼15 GPa). This figure is adapted from [37].

In the light alkali metals the d-bands play no role in Li and only a minor role in Na since they are located relatively far above the Fermi energy. Boettger and Trickey [21] concluded from their calculations for metallic Li that $s \rightarrow p$ transfer occurs under pressure, leading to an enhancement of n_p; for very strong compression, the bands near the Fermi surface also show an anomalous narrowing [21]. More recently, Neaton and Ashcroft have carried out a detailed analysis of the electronic structure of both Li [33] and Na [34] and conclude that radical deviations from nearly-free-electron behaviour occur at densities where the atomic core electrons begin to overlap, *i.e.* at pressures above 50 GPa for Li and 130 GPa for Na, including the possibility of a superconducting state. In figure 3 is shown the result of their calculation of the relative conduction electron density for Li at elevated pressures. Note how the conduction electrons are excluded from the ion cores and are forced to spend their time primarily in the *interstitial* regions of the lattice. In this case the translation of an alkali ion away from its equilibrium position would evidently have a particularly large effect on the valence electron states (strong electron–lattice interaction), a favorable situation for the appearance of superconductivity. At extremely high pressures, these authors predict that both Li and Na may enter a nearly insulating ground state where neighbouring cations pair up, as illustrated for Li in figure 3. Note that the paired-up cations have no strong chemical bond between them, but rather are pushed together by the high electron density in the interstitial

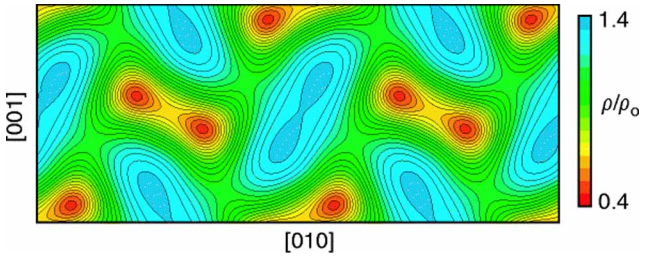

Figure 3. Relative charge density (see legend at right) of Li's 2s-conduction electrons for the *Cmca* structure at ∼100-GPa pressure. The Li^{1+}-ions are centred in the red regions; the conduction electron charge density is primarily concentrated in the blue interstitial regions. Reprinted by permission from Macmillan Publishers Ltd: [NATURE] J.B. Neaton and N.W. Ashcroft, Nature **400** 141 (1999), copyright (1999).

sites, *i.e.* a kind of 'forced marriage'. These results support the prediction of Siringo *et al.* [38] that under sufficient pressure the light alkali metals should be unstable to transitions to low-symmetry phases, possibly leading to a metal-insulator transition; interestingly, Angilella *et al.* [39] argue on general grounds that with increasing pressure the light alkali metals may actually oscillate back and forth between high-symmetry and low-symmetry structures.

As seen in figure 1, the alkali metals are extraordinarily compressible, almost as much as the molecular solid H_2, but clearly less than solid ^{3}He and ^{4}He. For example, a pressure of 184 GPa reduces the sample volume of Cs nearly *sevenfold* [40]. This leads to relatively large pressure-induced changes in all the solid state properties, including the crystal structure and electronic properties. It is thus not surprising that as the applied pressure is increased into the Mbar (100-GPa) range the alkali metals experience a plethoria of phase changes as seen in figure 4 as a function of both pressure and relative density. The $bcc \rightarrow fcc$ transition under pressure is universal among the alkalis, with, counterintuitively, transitions to lower-symmetry structures following at higher pressures. The reader is referred to an excellent review by

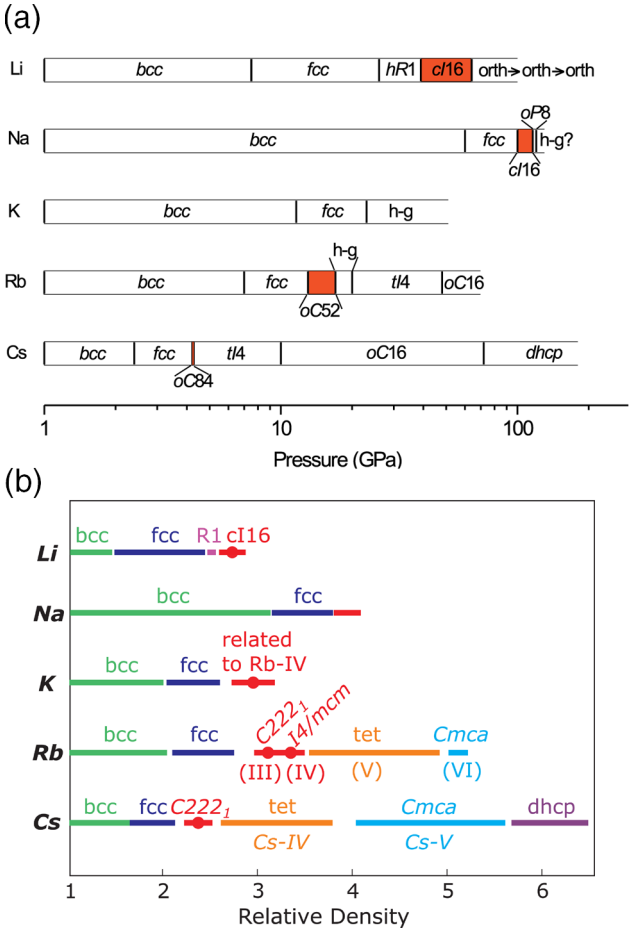

Figure 4. Stability range of different phases of a given alkali metal as a function of (upper) pressure to ∼100 GPa and (lower) relative density; in some cases different data sets were used in the upper and lower figures. Upper figure is reproduced with permission of IOP Publishing Ltd from: G.J. Ackland and I.R. Macleod, New J. Phys. **6** 138 (2004). Lower figure is a revised version of figure 2 from [40] provided courtesy of K. Syassen, I. Loa and M. Hanfland (copyright 2006). Structural data in lower figure on Li and Na were obtained in the temperature range 160–200 K, whereas those for K, Rb and Cs were determined at room temperature.

Syassen [40] for a full discussion of the structural changes in the alkali metals under pressure. We include more details in our discussion of the individual alkali metals below.

Measurements of the melting curves $T_M(P)$ of the alkali metals form an interesting extension of the structural phase diagrams where changes in crystal structure with pressure are signalled by abrupt changes in slope dT_M/dP. Unfortunately, the melting curves have only been studied over a limited pressure range for Li (8.0 GPa) [41], K (14.5 GPa) [42], Rb (14.0 GPa) [42] and Cs (8.0 GPa) [42]. Very recently the melting curve of Na has been determined to 118 GPa [43]. For all alkalis T_M initially increases with pressure, but passes through maxima in both the *bcc* and *fcc* phases for Na, Rb and Cs before passing through a minimum. For Na this minimum is particularly deep, falling at 118 GPa to 300 K, a temperature 71 K *lower* than its melting temperature at ambient pressure. It is notable that for all three alkalis this minimum occurs at a pressure near the transition from the high-symmetry *fcc* structure to one of lower symmetry, a pressure above which, in the case of Cs, superconductivity has been discovered [44, 45].

2. Results of experiment and theory

Of the five alkali metals studied in high-pressure experiments, only the heaviest and the lightest, Cs and Li, have been found to become superconducting. This fact, plus the similarity of the alkali structural phase diagrams in figure 4, would suggest that all alkali metals are likely to become superconducting under high pressure. Shi and Papaconstantopoulos [46] have recently carried out electronic structure calculations for Li, Na, K, Rb and Cs as a function of lattice parameter. They predict superconductivity for all alkali metals in the *fcc* structure where T_c increases with pressure; interestingly, for Na the predicted values of T_c are an order of magnitude lower than for the other alkali metals. Razzaque *et al.* [47] also predict superconductivity in Li's *fcc* phase under pressure where T_c increases steeply with decreasing sample volume. Further details of these and other theoretical calculations are included in the discussion below for the individual alkali metals.

2.1 *Cesium (Cs)*

The first alkali metal to become superconducting under high pressure is Cs. In 1970 Wittig [44] carried out quasihydrostatic pressure experiments using a pyrophyllite cell with steatite pressure medium and showed (see figure 5) that Cs becomes superconducting at $T_c \approx 1.3$ K for ~12-GPa pressure, T_c decreasing at higher pressures. Later experiments [45] to lower temperatures revealed superconductivity at 50 mK near 11 GPa in the Cs-IV phase, T_c initially increasing with pressure with a sudden jump to 1.3 K following the phase transition to Cs-V. From figure 1 it is seen that the pressure (~12 GPa) at the Cs-IV to Cs-V phase transition corresponds to $V/V_o \approx 0.25$ or a fourfold increase in atomic density, in agreement with the data in figure 4 (lower), yielding a molar volume of ~18 cm^3 $mole^{-1}$. According to [48] the $6s \rightarrow 5d$ transfer begins for Cs at $V/V_o \approx 0.5$ (~3 GPa) and ends at $V/V_o \approx 0.235$ (~15 GPa); at the pressure where superconductivity occurs, therefore, Cs's conduction electrons have taken on strong *d*-character, *i.e.* Cs has become a transition metal. In contrast to the expectations of Shi and Papaconstantopoulos [46], who estimated that *fcc*-Cs would superconduct near 3 K at 3 GPa, superconductivity in Cs thus appears to be associated with the Cs-IV (tetragonal) and Cs-V (*Cmca*) phases and *not* the *fcc* phase. We emphasize this result since, as we will see below, superconductivity in Li appears to be associated with the emergence of the *fcc* phase at low temperature. Note that in the pressure region where $s \rightarrow d$ transfer occurs (3–12 GPa), Cs is predominantly in the tetragonal phase. Superconductivity appears

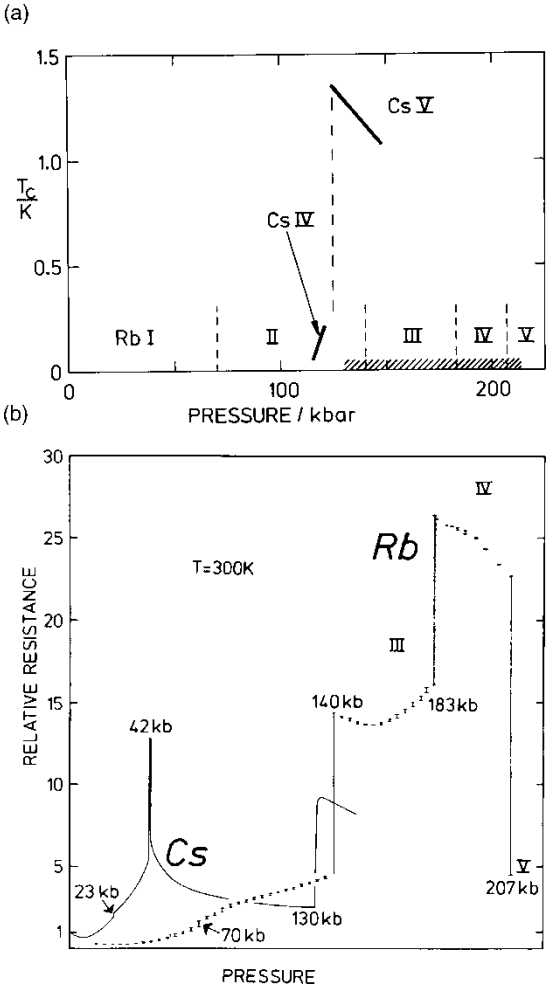

Figure 5. Upper: superconducting transition temperature T_c versus pressure for Cs. (100 kbar = 10 GPa.) T_c is seen to increase suddenly at the Cs-IV → Cs-V phase transition near 12 GPa. In Rb no superconductivity was found above 0.05 K in the pressure range 13–20.7 GPa (cross-hatched region). Lower: resistance at room temperature versus pressure for both Cs and Rb. Both figures taken from Wittig [45].

near the Cs-IV (tetragonal) → Cs-V (*Cmca*) transition. The *d*-character of the conduction electrons in Cs for pressures above 3 GPa may have a significant influence on its structural and superconducting transitions.

The electrical resistivity of Cs at room temperature has been measured as a function of pressure by several groups [49–51]. Of particular interest here are the resistivity studies of Wittig in figure 5 (lower) [51] where superconductivity in Cs was discovered at low temperatures, the first alkali metal to enter this exotic quantum state. To 20.7 GPa the resistivity shows a number of slope changes and breaks at the various crystallographic phase transitions, varying by more than an order of magnitude and passing through two prominent maxima near 4.2 and 13 GPa. The abrupt fivefold increase in the resistivity at 13 GPa would appear to be associated with the Cs-IV → Cs-V transition at which T_c jumps from approximately 0.2 to 1.3 K. This sharp increase in the room-temperature resistivity at the structural transition would be consistent with a strengthening of the electron–phonon interaction and thus an enhanced value of T_c.

It would be interesting to extend the above measurements of $T_c(P)$ on Cs to much higher pressures than 20 GPa using the most nearly hydrostatic pressure medium known, He. It is well known that the shear stresses generated by solid pressure media may seriously alter the measured $T_c(P)$ dependence [19, 20, 52, 53]. We will return to this point below when we discuss pressure-induced superconductivity in Li.

2.2 *Rubidium (Rb)*

Whereas the $6s \rightarrow 5d$ transfer in Cs is believed to be complete for $P \gtrsim 15$ GPa, pressures above 53 and 60 GPa, respectively, are required to complete the $5s \rightarrow 4d$ transfer in Rb and the $4s \rightarrow 3d$ transfer in K [48]. The fact that, as seen in figure 4, the phase diagrams of the heavy alkalis (particularly Cs and Rb) are closely similar suggests that the d-band occupancy n_d plays a role in determining the crystal structure. From Cs to K progressively higher pressures are required to stabilize a given crystal structure. Note that the Rb-V (tetragonal) $\rightarrow$ Rb-VI (*Cmca*) transition occurs at approximately the pressure (53 GPa) where the $s \rightarrow d$ transfer is completed; this behaviour was also exhibited by Cs. Based on the comparison with Cs, superconductivity in Rb is most likely to appear near 50 GPa. In addition, the melting curves of Cs, Rb and K are closely similar in the pressure range where they can be compared [42]. Shi and Papaconstantopoulos [46] estimate $T_c \approx 4$–8 K for *fcc*-Rb near 8-GPa pressure, depending on the value assumed for μ^*.

Unfortunately, no superconductivity has been observed in Rb above 50 mK over the pressure range $13 \leq P \leq 21$ GPa [45, 54]. However, we note from figures 4 and 5 that the maximum pressure of 21 GPa is very close to Rb's IV $\rightarrow$ V transition at room temperature; this is also seen in the electrical resistivity studies at ambient temperature where the IV $\rightarrow$ V transition is accompanied by a sharp decrease in the resistivity. It is thus not clear whether the Rb sample in these studies was actually in the Rb-V (tetragonal) phase at low temperatures where the search for superconductivity was carried out. Studies on Rb over a wider pressure range to pressures well above 20 GPa are thus recommended in a renewed search for superconductivity in this alkali metal.

2.3 *Potassium (K)*

In figure 4 it is seen that the *fcc* phase of K is stable at room temperature in the pressure range 11–23 GPa, above which transformation to a phase related to Rb-IV occurs. A transition to a tetragonal phase presumably occurs above 50 GPa with the *Cmca* phase appearing at higher pressure. Based on the analogy with Cs, the pressure region above 50 GPa is where superconductivity would be most likely to appear.

The *bcc* $\rightarrow$ *fcc* transition is clearly seen as an abrupt increase in the slope $\mathrm{d}T_M/\mathrm{d}P$ of the melting curve at 11 GPa; unfortunately, the melting curve was only determined to 15 GPa [42] so that the influence of the phase transitions at higher pressure on the melting curve remains unknown. Shi and Papaconstantopoulos [46] predict superconductivity in the range $T_c \approx$ 2–12 K for K's *fcc* phase near 14-GPa pressure, depending on the value assumed for μ^*. A recent first-principles electronic structure calculation for K by Sanna *et al.* [55, 56] predicts superconductivity in K's *fcc*-phase with T_c increasing from approximately 1 to 2 K as the pressure is increased from 21 to 23 GPa, increasing further to 11 K at 29 GPa after the transition into the K-III phase.

Deemyad *et al.* – see [57, 58] and S. Deemyad, V.G. Tissen and J.S. Schilling (unpublished) – carried out a search for superconductivity in K using a diamond-anvil cell loaded with helium pressure medium; no unequivocal evidence for a superconducting transition in K was obtained

over the temperature range 1.5–100 K for pressures of 3.6, 7.2, 9.7, 11 and 16.6 GPa nor for temperatures above 4 K at pressures of 4.7, 8.6, 12.9, 15.8, 20.8, 23.7, 26.8, 35.2, 37.0, 40.0, 42.5 and 43.5 GPa (for experimental details, see the discussion below under 'Li'). In a third experiment, a weak anomaly was observed near 1.7 K at 35 GPa that hinted at a possible superconducting transition – see [57] and V.G. Tissen (private communication); further studies are underway to check whether this anomaly is reproducible.

Here again, no evidence is found for superconductivity in K's fcc phase. We note that no evidence for superconductivity is found in the fcc phase for all three heavy alkali metals Cs, Rb and K. The lower-symmetry tetragonal or $Cmca$ phases appear to offer more fertile ground for superconductivity in these alkalis.

2.4 *Sodium (Na)*

Compared to the heavy alkali metals, pressure-induced $s \rightarrow p$ transfer is more important than $s \rightarrow d$ transfer in Li and Na since their d-bands lie relatively far above the Fermi energy. One might, therefore, anticipate that the high-pressure phase diagram and superconductivity in these two classes of alkali metals might differ substantially.

In figure 4 one sees that the lower-symmetry crystal structures that occur under pressure out of the fcc phase differ in the light and heavy alkalis; however, as pointed out by Ackland and Macleod [59], these structures are closely related. The stability range of the bcc phase in Na extends to much higher pressures ($\sim$65 GPa) than for the other alkali metals. A recent measurement of the melting curve of Na to 118 GPa shows that $T_{\mathrm{M}}(P)$ passes through a maximum of $\sim$1000 K near 30 GPa, exhibits a slope change at the $bcc \rightarrow fcc$ transition at 65 GPa, and passes through a deep minimum at 300 K immediately following the transition from fcc to a low-symmetry phase near 100 GPa [43]. Broadly similar behaviour in $T_{\mathrm{M}}(P)$ is exhibited by Cs and Rb; for Li and K data are not available to sufficiently high pressures to allow meaningful comparisons. This calls into question the importance of the presence or absence of $s \rightarrow d$ transfer in determining which phases occur in the alkali metals under high pressure. Ackland and Macleod [59] contend that Fermi-surface Brillouin zone interactions play a dominant role in accounting for the observed crystal structures.

Shi and Papaconstantopoulos [46] predict superconductivity for Na in the fcc phase, but at a much lower temperature ($\sim$0.2 K) than for the other alkali metals due to a 'delicate balance' between the pressure-dependent electronic and phononic terms; in contrast, the bcc phase is not predicted to be superconducting. In Na one would anticipate superconductivity above 65 GPa following the phase transition into the fcc phase, in analogy with the other light alkali metal, Li.

On the experimental side, Deemyad *et al.* – see [57, 58] and S. Deemyad, V.G. Tissen and J.S. Schilling (unpublished) – failed to detect any evidence for superconductivity above 4 K in an a.c. susceptibility measurement at the pressures 6.2, 17.4, 23.4, 25.7, 33.0, 38.0, 45.0, 52.5, 56.5 and 58.0 GPa (for experimental details, see the discussion below under 'Li'). The absence of superconductivity in this pressure range is not too surprising since, as seen in figure 4, Na remains in the bcc phase throughout this experiment to 58 GPa. The presence of the $bcc \rightarrow fcc$ transition at 65 GPa, the highly anomalous 'deep minimum' behaviour of Na's melting curve near 100 GPa and the transition from the fcc to a lower-symmetry phase at 100 GPa make a search for superconductivity in Na to pressures well above 60 GPa seem quite attractive. This is particularly true in view of the strong deviations from the nearly-free-electron model, ion pairing and semimetallic behaviour at elevated pressures predicted by Neaton and Ashcroft [34] for Na, as discussed in Section 1.

2.5 *Lithium (Li)*

Lithium may be the alkali metal with the most fascinating properties, at least until someone succeeds in metallizing hydrogen. Being the third lightest element in the periodic table, nearly 20 times lighter than Cs, it is not surprising that Li exhibits one of the highest values of T_c of all elemental superconductors. As has been emphasized by Boettger and Trickey [21] and Neaton and Ashcroft [33], the properties of Li become very non-free-electron-like under pressure as energy gaps open up and bands narrow, leading to low-symmetry crystal structures and highly anomalous electronic properties. Rodriguez-Prieto and Bergara [60] have extended such calculations to Li monolayers and predict interesting behaviour under pressure, including novel structural, electronic and even magnetic properties.

The first indication that Li becomes superconducting under pressure is seen in the electrical resistivity measurements carried out in 1986 by Lin and Dunn [61], which are reproduced in figure 6 (lower). The pressure technique was quasihydrostatic with solid boron nitride as pressure medium. A sharp break in the slope of the temperature-dependent resistance near 7 K at 22 GPa (220 kbar) does suggest the onset of a superconducting transition. The fact that the resistivity does not fall to zero is consistent with superconductivity for the two-point resistivity technique used. As the pressure increases above 22 GPa, the break in slope remains near 7 K, but the size of the resistance drop decreases, finally disappearing above 32 GPa. These results were reproduced in two further experimental runs. Lin and Dunn did not refer to possible superconductivity in Li in the title or abstract of their paper, but did state in the text of the manuscript that 'aside from Cs, this is the first time that a monovalent metal has indicated signs of possibly becoming superconducting at high pressures' [61]. The careful choice of words by the authors is to be commended; it is clear that Lin and Dunn should be recognized as being the first to give evidence for superconductivity in Li. Two other authors, Bednorz and Müller, carefully chose the words in the title of their landmark paper [62] which heralded the discovery of the superconducting cuprates 'Possible High T_c Superconductivity in the La–Ba–Cu–O System'.

The pressure dependence of the resistance of Li at room temperature in the studies of Lin and Dunn is shown in figure 6 (upper) [61]. The sudden resistance drop in the dashed line at 7 GPa (70 kbar) marks the $bcc \rightarrow fcc$ phase transition; according to Hanfland *et al.* [27] the fcc phase at 180 K extends up to pressures as high as 39 GPa. Lin and Dunn carried out a second experiment to nearly 30 GPa. As the pressure increases above 17 GPa, the sample resistance (solid line) in figure 6 (upper) is seen to increase strongly up to the maximum pressure of 30 GPa. This is the same pressure region where evidence for possible superconductivity appears, as seen in figure 6 (lower). In shock-wave studies Fortov *et al.* [63] observed a fifteenfold increase in the resistivity of Li as the pressure increases from 30 to 150 GPa.

Perhaps because of the emergence of high-temperature superconductivity in 1986, the results of Lin and Dunn remained widely underappreciated until 1999 when Neaton and Ashcroft published their important paper on 'Pairing in Dense Lithium' [33] where they confirmed the marked deviations from free-electron behaviour under pressure pointed out earlier by Boettger and Trickey [21] and predicted that in the pressure region near 100 GPa a paired orthorhombic structure $Cmca$ would be energetically favored over nine conventional monatomic structures; a possible superconducting state was also predicted. Neaton and Ashcroft [33] pointed out that the pairing is related to the Peierls transition in quasi 1D systems and arises from the strong increase in the pseudopotential at pressures sufficiently high to bring Li's small $1s$ electron core to partial overlap. The concomitant increase in the resistivity seen in figure 6 (upper) then arises from this enhancement of the pseudopotential.

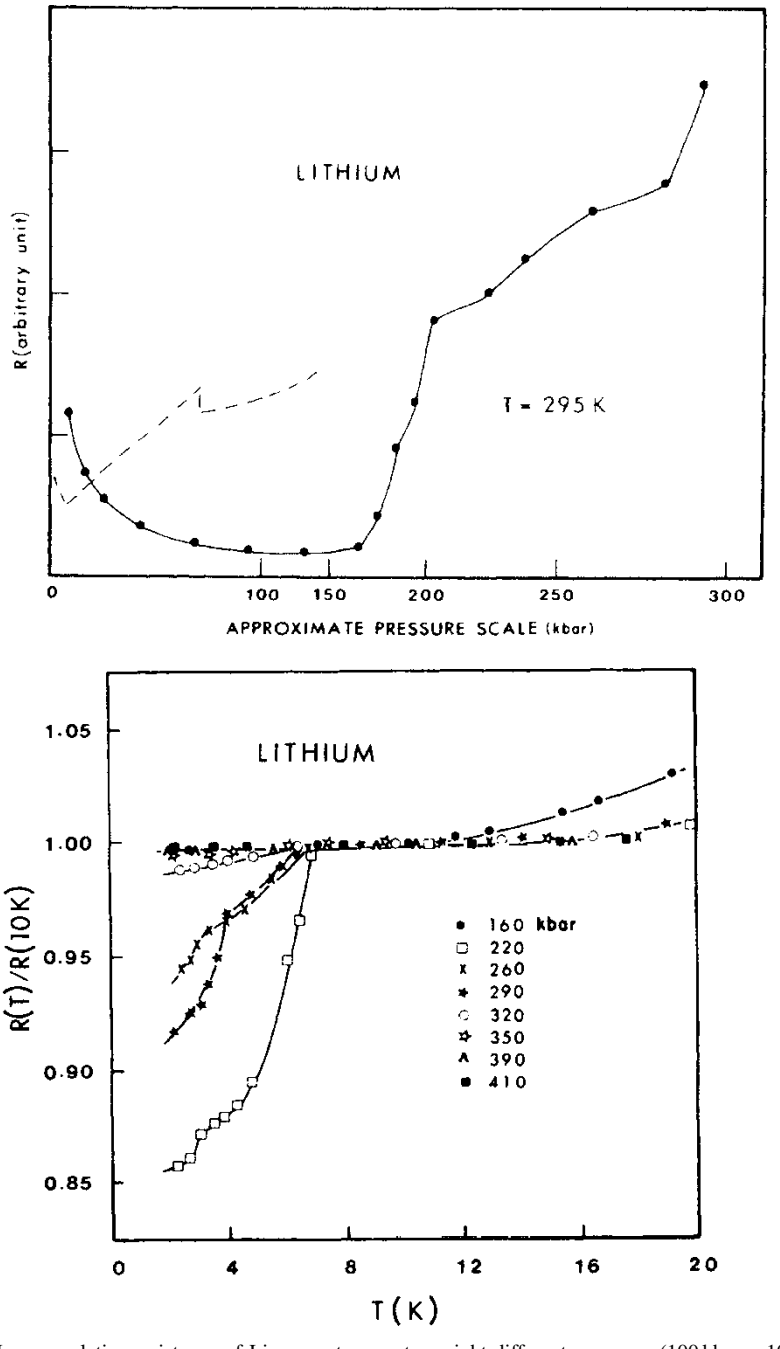

Figure 6. Lower: relative resistance of Li versus temperature eight different pressures (100 kbar = 10 GPa). For pressures in the range 22–32 GPa a sharp break in R(T) is seen near 7 K. Upper: resistance of Li versus pressure (100 kbar = 10 GPa) at room temperature. Drop in resistance near 7 GPa marks the $bcc \rightarrow fcc$ transition (dashed line). The resistance is seen to rise sharply (solid line) for pressures above 16 GPa. Both figures are taken from Lin and Dunn [61].

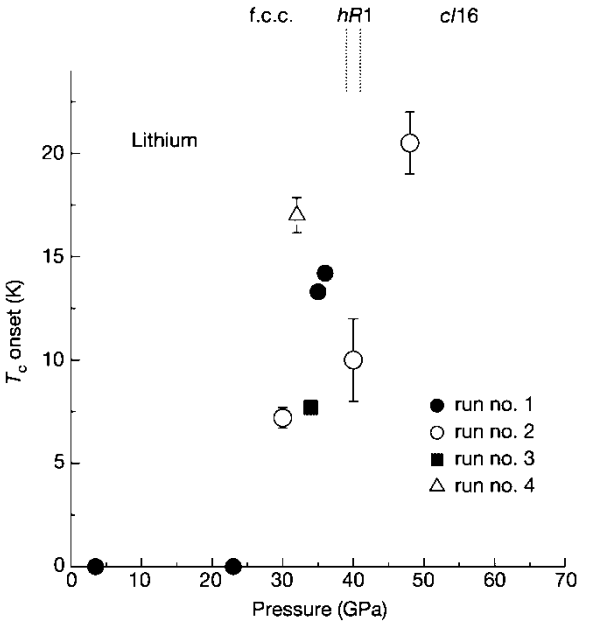

Figure 7. Superconducting transition temperature T_c of Li from the resistivity onset versus increasing pressure from four different experiments. Reprinted by permission from Macmillan Publishers Ltd: [NATURE] K. Shimizu, H. Ishikawa, D. Takao, T. Yagi and K. Amaya, Nature **419** 597 (2002), copyright (2002).

This paper set off a flurry of experimental activity to search for both the predicted paired state and possible superconductivity. One year later, in 2000, synchrotron X-ray diffraction studies to 50 GPa at temperatures near 200 K by Hanfland *et al.* [27, 40] revealed the well known $bcc \rightarrow fcc$ transition near 7.5 GPa followed by a transition at 39.8 GPa to a rhombohedral $hR1$ structure and then at 42.5 GPa to a structure never observed before for any other element, one with a $cI16$ cubic symmetry. The search is still on for the paired structure envisioned by Neaton and Ashcroft [33] at higher pressures.

Finally, in 2002 Shimizu *et al.* [64] found evidence for superconductivity above 20 GPa in electrical resistivity measurements on Li to 48 GPa, shown in figure 7, where T_c is defined by the resistivity onset. The sample was trapped in a pit in one of the diamond anvils; no pressure medium was used. The resistivity transitions themselves are quite broad, extending, for example, at 48-GPa pressure from onset at 20 K to midpoint at 10 K; this gives evidence for sizeable pressure and/or phase inhomogeneity. The T_c values in figure 7 are the accumulated results from four separate experiments. With increasing pressure, T_c determined from the resistivity onset shifts rapidly to higher temperatures, reaching 20 K at 48 GPa. The agreement between the $T_c(P)$ data from the different runs is rather poor. These authors confirmed that the resistivity transition shifts to lower temperatures with increasing magnetic field, the expected behaviour for a superconductor. The results of Shimizu *et al.* [64] thus confirm the earlier suspicions of Lin and Dunn [61] that Li becomes superconducting at pressures above 20 GPa.

A more definitive proof of superconductivity in Li at high pressure was given somewhat later in 2002 by Struzhkin *et al.* [65] in their a.c. susceptibility measurements (two runs) on Li to 40 GPa and resistivity measurements (one run) in the pressure range 42–84 GPa, as shown in figure 8. No pressure medium was used. T_c is defined by the resistivity or susceptibility onset temperature. The resistivity transitions are 5–10 K wide, depending on the pressure; the susceptibility transitions are narrower $\sim$2 K. It is well known that the resistivity onset normally

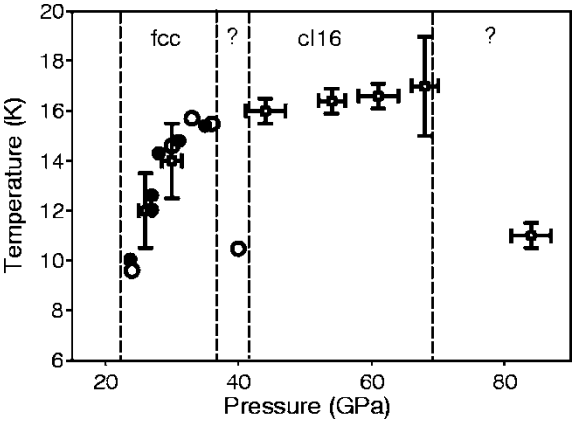

Figure 8. Superconducting transition temperature T_c of Li versus increasing pressure from the a.c. susceptibility onset (two experiments) to 40 GPa and from the resistivity onset to higher pressures. Reprinted with permission from V.V. Struzhkin, M.I. Eremets, W. Gan, H.-K. Mao, R.J. Hemley, Science **298** 1213 (2002). Copyright 2002 AAAS.

yields higher values of T_c than the susceptibility onset or susceptibility midpoint (see, for example, [66]), although this is not evident from the overlaping resistivity/susceptibility data in figure 8 near 30 GPa. The pressure dependence of T_c in figure 8 confirms that Li becomes superconducting somewhat above 20 GPa, with T_c increasing initially rapidly with pressure. The T_c value from the a.c. susceptibility data at 40 GPa lies at a relatively low temperature. For pressures in the range 40–70 GPa, the resistivity data show a nearly constant $T_c(P)$, the final data point at 84 GPa lying markedly lower. Both anomalously low data points at 40 and 84 GPa are indicative of structural phase transitions.

Although the three high-pressure experiments on Li discussed so far [61, 64, 65] agree that Li becomes superconducting above 20 GPa, there is relatively poor agreement at higher pressures. This can arise from differences in the samples, pressure techniques, or measurement techniques used. In none of these studies was a particularly large set of $T_c(P)$ data points accumulated. In view of the fact that either no pressure medium [64, 65] or the hard solid BN [61] was used as pressure medium, it is certainly possible that the measured $T_c(P)$ dependences in figures 6–8 were influenced by shear stress effects. However, the sudden appearance of superconductivity near 20 GPa appears to be a robust feature on which all three experiments agree. Shear stress effects on $T_c(P)$ have been well documented [19, 20]. Sizoo and Onnes [67] reported that T_c for Sn or In decreases under hydrostatic pressure, but increases if uniaxial pressure is applied. β-Hg, a shear-stress-induced body-centred tetragonal modification of ordinary rhombohedral α-Hg, exhibits distinctly different superconducting properties [68]. Further examples of shear stress effects and widely differing hydrostatic versus uniaxial pressure effects on superconductivity are given in [19, 20, 52, 53].

For these reasons we set out to determine the superconducting phase diagram of Li using the most hydrostatic pressure medium available, helium. Care was taken that the Li sample did not come into close contact with either the diamond anvils or the rhenium gasket during the entire experiment; as in previous structural studies [27], the temperature of the diamond-anvil cell was kept below 200 K to reduce the chance of the Li sample reacting with the diamond anvils or gasket.

In figure 9 (left) is shown the coil arrangement used for a.c. susceptibility measurements in the non-magnetic BeCu diamond-anvil cell. Two identical coils are shown wound with 60 μm Cu wire consisting of an outer primary coil (130 turns) and an inner secondary coil (180 turns). One coil is placed around the lower diamond anvil (1/6 carat, 0.5-mm diameter culet with

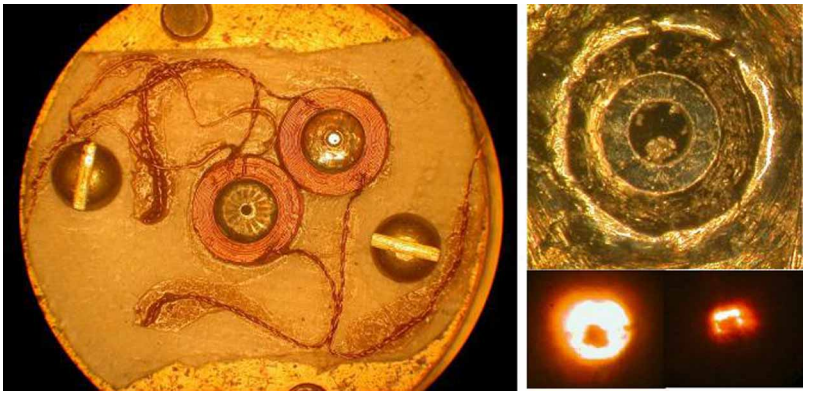

Figure 9. Left: the arrangement of measuring and compensating coils in the diamond-anvil cell used in the experiments on Li. Right-top: Au-plated Re gasket with a 250 μm bore containing the Li sample and ruby spheres. Right-bottom: a transmitted light photograph of cell at (left) ambient pressure and (right) 30-GPa pressure. Figure is taken from Tomita *et al.* [58] with permission of IOP Publishing Limited.

no bevel) with the compensating coil directly adjacent. A preindented gold-plated Re gasket is placed in both measuring and compensating coils to reduce the background signal in the a.c. susceptibility. In figure 9 (right upper) a top view of the preindented gasket is given; in the 0.25-mm diameter hole are seen the tiny Li sample at the bottom and clumps of ruby spheres at the top which serve as an internal manometer. Before applying pressure, liquid He is filled into the gasket hole to serve as a nearly hydrostatic pressure medium. In figure 9 (right lower) the transmitted light photos show the sample and hole at both ambient pressure (left) and 30-GPa pressure (right). From the equation of state of Li in figure 1 we see that 30-GPa pressure reduces the sample volume by somewhat more than a factor of two; this strong reduction in sample size is clearly seen in the figure. Further experimental details are given in [52].

In figure 10 the temperature dependence of the real part of the a.c. susceptibility is shown for Li at various pressures between 20.3 and 61.7 GPa. The negative downturn (10–20 nV) in the a.c. susceptibility is clearly seen, signalling the superconducting transition. The pressure dependence of T_c is evidently strongly non-monotonic. The full superconducting phase diagram $T_c(P)$ for Li is shown in figure 11 to nearly hydrostatic pressures as high as 67 GPa [52] for both increasing and decreasing pressure with over 30 data points; $T_c(P)$ is seen to be quite reversible.

There are significant differences between the phase diagram in figure 11 and those from the previous studies in figures 6–8, particularly above 40 GPa. Under nearly hydrostatic pressure Li is seen in figure 11 to become superconducting at ∼5 K for 20 GPa, T_c increasing initially rapidly with pressure to ∼14 K at 30 GPa. The phase analysis of Lin and Dunn [61] would suggest that the sudden appearance of superconductivity at 20 GPa is related to the suppression under pressure of the well-known phase transition from fcc to a lower-symmetry 9R structure at low temperature. Li's superconductivity in the pressure range 20–30 GPa is thus believed to be associated with the fcc structure. As the pressure increases above 30 GPa, a structural phase transition appears to occur as evidenced by the sharp break in slope dT_c/dP changing from positive to negative values (note the additional broadening of the superconducting transition in this region). At higher pressures, $T_c(P)$ passes through a minimum near 50 GPa and rises steeply before dropping suddenly below 4 K at 67 GPa. Although it is possible that at or above 67 GPa Li has transformed into the paired semiconducting state envisioned by Neaton and Ashcroft [33], we have no clear evidence for this. Exposing the Li sample where $T_c \approx 6$–8 K

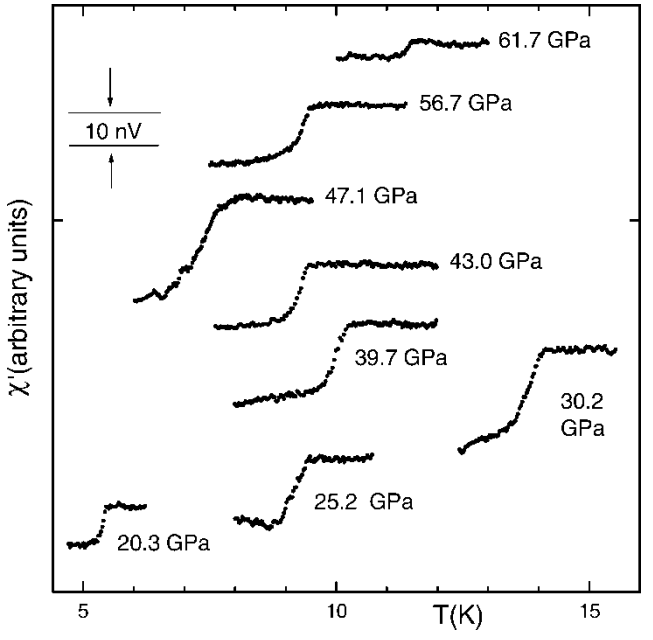

Figure 10. Superconducting transition of Li in the real part of the a.c. susceptibility for eight values of nearly hydrostatic (He pressure medium) pressure. Figure is taken from Deemyad *et al.* [52]. The midpoint of the transition determines T_c.

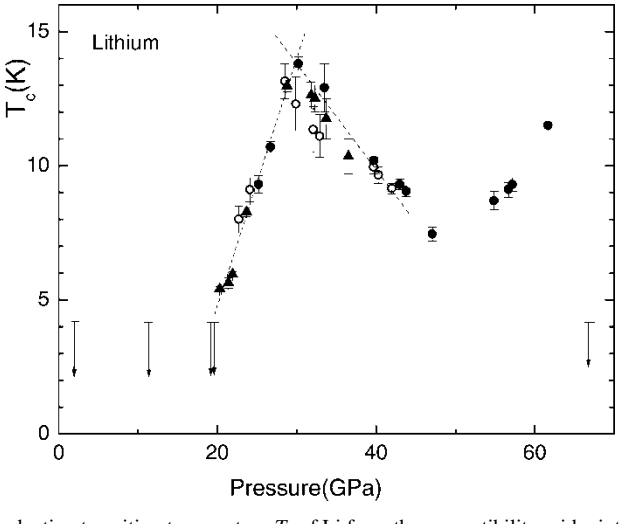

Figure 11. Superconducting transition temperature T_c of Li from the susceptibility midpoint versus nearly hydrostatic pressure; run 1 increasing (•) and decreasing (○) pressure, run 2 increasing pressure (▲). Figure is taken from Deemyad *et al.* [52].

to a d.c. magnetic field of ∼200 Oe results in a rapid decrease in T_c, similar to that for Pb, thus giving evidence that superconducting Li is a type I superconductor [52].

Experiments to pressures in the Mbar region which examine Li's magnetic, electrical and optical properties would be very interesting.

3. Conclusions

We would now like to search for a simple criterion for the appearance of superconductivity in a given alkali metal under pressure. After considering carefully the crystal structures taken on by the fourteen elements across the rare-earth series, Johansson and Rosengren [69] pointed out in 1975 that the ratio of the Wigner–Seitz radius to ionic radius, r_a/r_c, appears to play an important role in determining their equilibrium crystal structure sequence *hcp* $\rightarrow$ Sm-type $\rightarrow$ *dhcp* $\rightarrow$ *fcc*. This sequence is followed either progressing from right to left across the series or upon applying high pressure to a given rare-earth metal. Why is this? Almost all rare earths are trivalent in a solid so that the character of their conduction electrons is derived from 6*s* and 5*d* atomic states. As emphasized by Duthie and Pettifor [35] (see Section 1), the *d*-band occupancy, n_d, is the principal factor determining the crystal structure; n_d increases when high pressure is applied owing to $s \rightarrow d$ transfer. Since n_d is inversely related to the free volume available to the conduction electrons [35], a measure of which is the ratio r_a/r_c which decreases under pressure, one would anticipate a correlation between the ratio r_a/r_c and the rare-earth crystal structure sequence.

It is interesting that under pressures to $\sim$50 GPa several trivalent transition metals also follow related crystal structure sequences: Y (*hcp* $\rightarrow$ Sm-type $\rightarrow$ *dhcp* $\rightarrow$ *trigonal*) [70, 71], Lu (*hcp* $\rightarrow$ *Sm-type*) [71], La (*dhcp* $\rightarrow$ *fcc* $\rightarrow$ trigonal) [71] and Sc (*hcp* $\rightarrow$ β-Np) [71]. Johansson and Rosengren [69] also demonstrated a relationship between the pressure-dependent superconducting properties of the trivalent transition metal systems Y, La, Lu and La–Y, La–Lu alloys and the decreasing value of the ratio r_a/r_c under pressure. A plot of T_c versus r_a/r_c for the trivalent transition metal systems Y, La, Sc and Lu in figure 12 reveals that no superconductivity exists if the ratio r_a/r_c is too large. Decreasing r_a/r_c to values under 2.1 by applying pressure is seen to enhance the values of T_c to above 1 K. Since for La the ratio is $r_a/r_c \leq 2.1$ at ambient pressure it is not surprising that La is indeed superconducting at 6 K; with increasing pressure T_c passes through a maximum. In contrast, for Y T_c increases monotonically with pressure to nearly 20 K at 115 GPa where $r_a/r_c = 1.65$ – see [72] and J.J. Hamlin, V.G. Tissen and J.S. Schilling (unpublished). The maximum pressure applied by Wittig [73] to Sc (21 GPa) yields $r_a/r_c = 2.25$ and is insufficient to raise T_c above 0.35 K. However, very recent studies under nearly hydrostatic pressure to 74 GPa have succeeded in pushing T_c for Sc up to 8.1 K – see J.J. Hamlin and J.S. Schilling (unpublished).

Does a similar correlation exist for the alkali metals between the ratio r_a/r_c and their crystal structures or superconductivity? Alkali metals differ markedly from the trivalent transition metals. All alkali metals remain monovalent under Mbar pressures; however, the heavy alkalis Cs, Rb and K eventually become transition metals under pressure due to $s \rightarrow d$ transfer, whereas the light alkalis Na and Li exhibit mainly $s \rightarrow p$ transfer. As seen in figure 4, there appear to indeed be differences in the structure sequences under pressure between the heavy and light alkalis: the light alkalis don't show the tetragonal structure of Rb-V or Cs-IV, whereas the heavy alkalis don't take on the *R*1 or *cI*16 structures of Li. Exploring the phase diagrams to even higher pressures will allow a more complete assessment of possible correlations between the structural sequences of all alkali metals under pressure. Ackland and Macleod [59] discuss a theory for the observed structural sequences of the alkalis under pressure on the basis of a nearly-free-electron picture where the most important contribution to the crystal structure arises from Fermi-surface Brillouin zone interactions.

Let us now examine figure 12 for possible correlations in the alkali metals between T_c and the ratio r_a/r_c. Surprisingly, the lightest alkali, Li, does appear to fit into the scheme of the trivalent transition metals. Li's ambient pressure value of $r_a/r_c \simeq 2.28$ places it well to the right in the non-superconducting region. However, as seen in figure 11, Li becomes superconducting

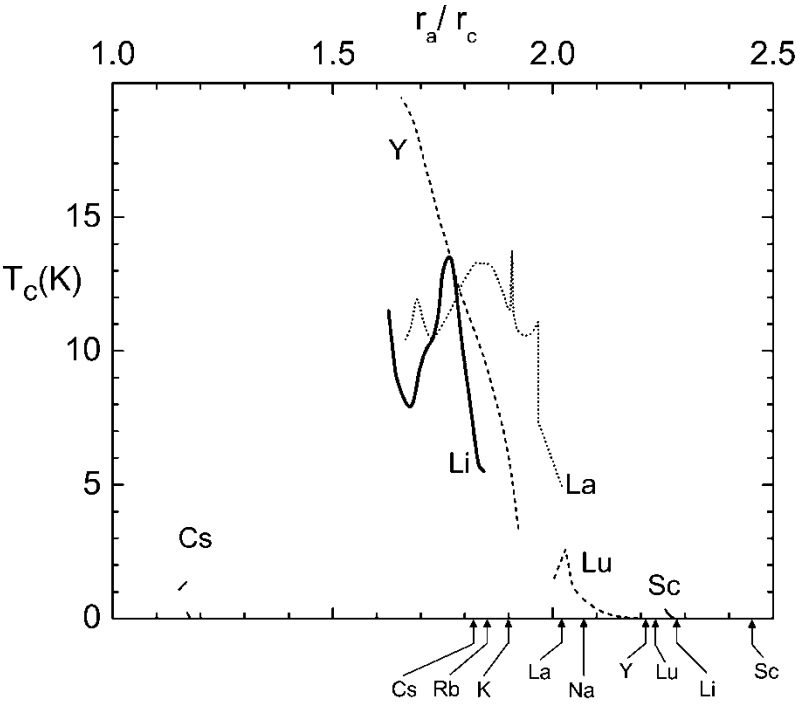

Figure 12. Value of T_c versus ratio of Wigner–Seitz radius to ionic radius, r_a/r_c, for Y – see [72] and J.J. Hamlin, V.G. Tissen and J.S. Schilling (unpublished) – Sc [73], La [74], Lu [75], Li [52] and Cs [44, 45]. The values of the ratio r_a/r_c at ambient pressure, as indicated by the vertical arrows at the bottom of the figure, are: Y (2.21), Lu (2.23), Sc (2.45), La (2.02), Li (2.28), Na (2.07), K (1.90), Rb (1.85) and Cs (1.82). (Values of the ionic radius r_c and volume per atom V_a at ambient pressure are taken from [36]. For Y^{3+}, Sc^{3+}, La^{3+}, Lu^{3+}, Li^{1+}, Na^{1+}, K^{1+}, Rb^{1+}, Cs^{1+} we find, respectively, $r_c = 0.90$, 0.75, 1.03, 0.86, 0.76, 1.02, 1.38, 1.52, 1.67 Å and $r_a \equiv \sqrt[3]{(3/4\pi)V_a)} = 1.99$, 1.84, 2.08, 1.92, 1.73, 2.11, 2.62, 2.81, 3.04 Å.)

near 5 K at 20 GPa and T_c increases initially rapidly with pressure, not unlike the steep climb for the transition metal Y. Phase transitions in Li lead to a complicated $T_c(P)$ dependence for $P \geq 30$ GPa. In contrast, the superconductivity of the heavy alkali metal Cs does not fit into the above scheme. Cs's ambient pressure value $r_a/r_c \simeq 1.82$ is less than the values for Sc, Lu, La and Y where they superconduct; in fact, for La and Y T_c lies at relatively high temperatures above 10 K. Superconductivity in Cs first appears for $r_a/r_c < 1.2$! The absence of superconductivity in Rb, K and Na under pressure also doesn't fit into the scheme of figure 12 whereby superconductivity should appear above 1 K for $r_a/r_c \leq 2.1$. No superconductivity was observed for Rb (above 0.05 K up to 21 GPa where $r_a/r_c \simeq 1.23$), for K (above 1.5 K up to 16.6 GPa where $r_a/r_c \simeq 1.41$ or above 4 K up to 43.5 GPa where $r_a/r_c \simeq 1.26$), or for Na (above 4 K up to 58 GPa where $r_a/r_c \simeq 1.42$). If there is any correlation between T_c and the ratio r_a/r_c for the alkali metals, it is a good deal more complex than that for the trivalent transition metals. This is not completely unexpected since the change in properties of the alkalis under pressure is fundamental in nature and far more extreme due in part to their much larger compressibility. Nevertheless, it is likely that all alkali metals will become superconducting at sufficiently high pressure. The observation of superconductivity in more of the alkali metals would allow a more meaningful search for possible correlations between T_c and r_a/r_c.

From the preceding it is clear that a great deal of exciting new physics is created in the alkali metals when sufficient pressure is applied that the atomic cores begin to overlap. Compared to other non-alkali simple metal or transition metal systems, this occurs at relatively modest

pressures owing to the very high compressibility of the alkali metals (see figure 1). As pointed out by Neaton and Ashcroft [34], the conclusion that the conduction electronic states become highly anomalous when the core states begin to overlap is quite general. Perhaps some day even the noble metals will become superconducting if their purity and the applied pressure are both sufficiently high.

Acknowledgements

The author would like to express his appreciation to N. Ashcroft, S. Deemyad, J. Hamlin and W. Pickett for critically reading the first draft of this paper. Thanks are due J. Hamlin for technical support and K. Syassen for providing the revised alkali phase diagram in figure 4 (lower). The author also gratefully acknowledges the support of the National Science Foundation through grant DMR-0404505.

References

[1] N.W. Ashcroft, Phys. Rev. Lett. **21** 1748 (1968).
[2] D.R. Lide (Editor-in-Chief), *CRC Handbook of Chemistry and Physics* 85th edn, 2004–2005 (CRC Press, NY, 2004), pp. 4–12.
[3] J.E. Simsarian, A. Ghosh, G. Gwinner, L.A. Orozco, G.D. Sprouse and P.A. Voytas, Phys. Rev. Lett. **76** 3522 (1996).
[4] E. Babaev, A. Sudbø and N.W. Ashcroft, Nature **431** 666 (2004).
[5] E. Babaev, A. Sudbø and N.W. Ashcroft, Phys. Rev. Lett. **95** 105301 (2005).
[6] E. Smørgrav, E. Babaev, J. Smiseth and A. Sudbø, Phys. Rev. Lett. **95** 13501 (2005).
[7] C. Narayana, H. Luo, J. Orloff, A.L. Ruoff, Nature **393** 46 (1998).
[8] P. Loubeyre, F. Occelli and R. LeToullec, Nature **416** 613 (2002).
[9] S.A. Bonev, E. Schwegler, T. Ogitsu and G. Galli, Nature (London) **431** 669 (2004).
[10] S.T. Weir, A.C. Mitchell and W.J. Nellis, Phys. Rev. Lett. **76** 1860 (1996).
[11] A. Israel and Y.K. Vohra, Mater. Res. Soc. Symp. Proc. **499** 179 (1998).
[12] R. Hemley and C.-S. Yan, *Very Large Diamonds Produced Very Fast* (Carnegie Institution, Washington, DC, 16 May 2005), press release.
[13] N.W. Ashcroft, Phys. Rev. Lett. **92** 187002 (2004).
[14] J. Feng, W. Grochala, T. Jaroń, R. Hoffmann, A. Bergara and N.W. Ashcroft, Phys. Rev. Lett. **96** 017006 (2006).
[15] E. Wigner and F. Seitz, Phys. Rev. **43** 804 (1933).
[16] A. Liu and M. Cohen, Phys. Rev. B **44** 9678 (1991).
[17] C.F. Richardson and N.W. Ashcroft, Phys. Rev. B **55** 15130 (1997).
[18] K.I. Juntunen and J.T. Tuoriniemi, Phys. Rev. Lett. **93** 157201 (2004).
[19] J.S. Schilling, in *Treatise on High Temperature Superconductivity*, edited by J.R. Schrieffer (Springer Verlag, Hamburg, 2006).
[20] J.S. Schilling and S. Klotz, in *Physical Properties of High Temperature Superconductors*, edited by D.M. Ginsberg, Vol. III (World Scientific, Singapore, 1992), p. 59.
[21] J.C. Boettger and S.B. Trickey, Phys. Rev. B **32** 3391 (1985).
[22] A. Rodriguez-Prieto and A. Bergara, in *Proceedings of the Joint 20th AIRAPT/43rd EHPRG*, 27 June–1 July 2005, Karlsruhe, Germany.
[23] A. Bergara, A. Rodriguez-Prieto and V.M. Silkin, BAPS U42.00006, 13–17 March 2006, Baltimore, Maryland.
[24] P. Loubeyre, R. LeToullec, D. Hausermann, M. Hanfland, R.J. Hemley, H.K. Mao and L.W. Finger, Nature **383** 702 (1996).
[25] J. van Straaten, R.J. Wijngaarden and I.F. Silvera, Phys. Rev. Lett. **48** 97 (1982)
[26] M. Hanfland, I. Loa, K. Syassen, U. Schwarz and K. Takemura, Solid State Commun. **112** 123 (1999).
[27] M. Hanfland, K. Syassen, N.E. Christensen and D.L. Novikov, Nature **408** 174 (2000).
[28] M. Hanfland, I. Loa and K. Syassen, Phys. Rev. B **65** 184109 (2002).
[29] M. Winzenick, V. Vijayakumar and W.B. Holzapfel, Phys. Rev. B **50** 12381 (1994).
[30] K. Takemura, N.E. Christensen, D.L. Novikov, K. Syassen, U. Schwarz and M. Hanfland, Phys. Rev. B **61** 14399 (2000).
[31] K. Takemura and K. Syassen, Phys. Rev. B **32** 2213 (1985).
[32] A. Dewaele, P. Loubeyre and M. Mezouar, Phys. Rev. B **70** 094112 (2004).
[33] J.B. Neaton and N.W. Ashcroft, Nature **400** 141 (1999).
[34] J.B. Neaton and N.W. Ashcroft, Phys. Rev. Lett. **86** 2830 (2001).
[35] J.C. Duthie and D.G. Pettifor, Phys. Rev. Lett. **38** 564 (1977).
[36] W. Martienssen and H. Warlimont (Editors), *Springer Handbook of Condensed Matter and Materials Data* (Springer-Verlag, Berlin, 2005).

[37] R. Grover, A.K. McMahan and M. Ross, Europhys. Conf. Abstracts **1A** 18 (1975).
[38] F. Siringo, R. Pucci, and G.G.N. Angilella, High Pressure Research **15** 255 (1997).
[39] G.G.N. Angilella, F. Siringo, and R. Pucci, Eur. Phys. J. B **32** 323 (2003).
[40] K. Syassen, *Proc. Int. School of Physics Enrico Fermi Course CXLVII*, edited by R.J. Hemley *et al.* (IOS Press, Amsterdam, 2002), p. 251.
[41] H.D. Luedemann and G.C. Kennedy, J. Geophys. Res. **73** 2795 (1968).
[42] R. Boehler and C.-S. Zha, Physica **139 & 140B** 233 (1986).
[43] E. Gregoryanz, O. Degtyareva, M. Somayazulu, R.J. Hemley and H.-K. Mao, Phys. Rev. Lett. **94** 185502 (2005).
[44] J. Wittig, Phys. Rev. Lett. **24** 812 (1970).
[45] J. Wittig, in *Superconductivity in d- and f-Band Metals*, edited by W. Buckel and W. Weber (Kernforschungszentrum, Karlsruhe, 1982), p. 321–29.
[46] L. Shi and D.A. Papaconstantopoulos, Phys. Rev. B **73** 184516 (2006).
[47] A. Razzaque, A.K.M.A. Islam, F.N. Islam and M.N. Islam, Solid State Commun. **131** 671 (2004).
[48] A.K. McMahan, Phys. Rev. B **29** 5982 (1984).
[49] P.W. Bridgman, Proc. Am. Acad. Arts Sci. **81** 165 (1952).
[50] R.A. Stager and H.G. Drickamer, Phys. Rev. Lett. **12** 19 (1964).
[51] J. Wittig, Mat. Res. Soc. Symp. Proc. **22** 17 (1984).
[52] S. Deemyad and J.S. Schilling, Phys. Rev. Lett. **91** 167001 (2003)
[53] I.V. Aleksandrov, A.F. Goncharov, I.N. Makarenko and S.M. Stishov, Phys. Rev. B **43** 6194 (1991).
[54] K. Ullrich, C. Probst and J. Wittig, J. de Physique, Colloque **1** 463 (1978).
[55] A. Sanna, C. Franchini, A. Floris, G. Profeta, N.N. Lathiotakis, M. Lüders, M.A.L. Marques, E.K.U. Gross, A. Continenza and S. Massidda, Phys. Rev. B **73** 144512 (2006).
[56] G. Profeta, C. Franchini, N.N. Lathiotakis, A. Floris, A. Sanna, M.A.L. Marques, M. Lüders, S. Massidda, E.K.U. Gross and A. Continenza, Phys. Rev. Lett. **96** 047003 (2006).
[57] S. Deemyad, PhD thesis, Washington University in St. Louis (2004).
[58] T. Tomita, S. Deemyad, J.J. Hamlin, J.S. Schilling, V.G. Tissen, B.W. Veal, L. Chen and H. Claus, J. Phys.: Condens. Matter **17** S921 (2005).
[59] G.J. Ackland and I.R. Macleod, New J. Phys. **6** 138 (2004).
[60] A. Rodriguez-Prieto and A. Bergara, Phys. Rev. B **72** 125406 (2005).
[61] T.H. Lin and K.J. Dunn, Phys. Rev. B **33** 807 (1986).
[62] J.G. Bednorz and K.A. Müller, Z. Phys. B **64** 189 (1986).
[63] V.E. Fortov, V.V. Yakushev, K.L. Kagan, I.V. Lomonosov, E.G. Maksimov, M.V. Magnitskaya, V.I. Postnov and T.I. Takusheva, J. Phys.: Condens. Matter **14** 10809 (2002).
[64] K. Shimizu, H. Ishikawa, D. Takao, T. Yagi and K. Amaya, Nature **419** 597 (2002).
[65] V.V. Struzhkin, M.I. Eremets, W. Gan, H.-K. Mao and R.J. Hemley, Science **298** 1213 (2002).
[66] R. Lortz, T. Tomita, Y. Wang, A. Junod, J.S. Schilling, T. Masui and S. Tajima, Physica C **434** 194 (2006).
[67] G.J. Sizoo and H.K. Onnes, Commun. Phys. Lab. Univ. Leiden, No. 180b (1925).
[68] J.E. Schirber and C.A. Swenson, Phys. Rev. **123** 1115 (1961).
[69] B. Johansson and A. Rosengren, Phys. Rev. B **11** 2836 (1975).
[70] Y.K. Vohra, H. Olijnik, W. Grosshans and W.B. Holzapfel, Phys. Rev. Lett. **47** 1065 (1981).
[71] W.A. Grosshans and W.B. Holzapfel, Phys. Rev. B **45** 5171 (1992).
[72] J.J. Hamlin, V.G. Tissen and J.S. Schilling, Phys. Rev. B **73** 094522 (2006).
[73] J. Wittig, C. Probst, F.A. Schmidt and K.A. Gschneidner Jr, Phys. Rev. Lett. **42** 469 (1979).
[74] V.G. Tissen, E.G. Ponyatovskii, M.V. Nefedova, F. Porsch and W.B. Holzapfel, Phys. Rev. B **53** 8238 (1996).
[75] C. Probst and J. Wittig, in *Handbook on the Physics and Chemistry of Rare Earths*, edited by K.A. Gschneidner Jr and L. Eyring (North-Holland, Amsterdam, 1978), p. 749.